Table 1 Comparison between approximate (η_0) and exact (η) equations for fin effect; $\theta_1 = 0$

$\nu \equiv k_f R/k_w t$	η	η_0	η/η_0
0.001	0.993	0.993	1.0
0.003	0.979	0.979	1.0
0.01	0.934	0.934	1.0
0.03	0.826	0.829	0.997
0.1	0.599	0.613	0.978
0.3	0.360	0.389	0.926
1.	0.1864	0.2155	0.865
3.	0.1111	0.1244	0.893
10.	0.0726	0.0682	1.065
30.	0.0543	0.0393	1.38
100.	0.0423	0.0216	1.96
1000.	0.0297	0.0068	4.36

coefficient can be evaluated from the usual theory, giving $h = h_0$. The fin effect of the tube wall can be incorporated into the analysis by use of the straight-fin effectiveness[6];

$$\eta_0 = [\tanh(h_0 L_f^2/k_w t)^{1/2}]/(h_0 L_f^2/k_w t)^{1/2} \quad (15)$$

For $\theta_1 = 0$, $L_f = \pi R$. Since[6] $h_0 = 48k_f/(22R)$

$$\eta_0 = [\tanh(24\pi^2\nu/11)^{1/2}]/(24\pi^2\nu/11)^{1/2} \quad (16)$$

The values of η and η_0 are compared in Table 1. In practice, ν might range from 0.001 for dielectric fluids in small aluminum tubes to 100 for liquid metals in large stainless-steel tubes. In the latter case, the flow is more likely to be turbulent, so applicability of the laminar flow solution is probably limited to low values of ν, where $\eta_0 \simeq \eta$.

Conclusions

An analytical model has been developed to predict the effects of circumferential wall-temperature gradients in spacecraft radiator tubes. Exact solutions have been derived for the fin effectiveness of the tube wall in terms of an infinite system of linear equations. A convenient expression has been derived for the extreme case of point contact between tube wall and radiating fin. An approximate solution, based on neglecting the conduction-convection interaction, has been derived for the same analytical model; it compares favorably with the exact solution for $(k_f R/k_w t) < 3$, which should include most cases of interest in environmental-control systems. For cases in which a larger contact region must be considered, so that the fin length is less than that for point contact, the approximate solution should give even more accurate results.

Similar analyses might be conducted for turbulent flow, using the hypothesis that the circumferential eddy diffusivity equals the radial eddy diffusivity.[7]

References

[1] Lubin, B. T. and Trusch, R. B., "Prediction of Space Radiator Performance," Paper 63-AHGT-85, 1963, American Society of Mechanical Engineers.

[2] Sparrow, E. M., Johnson, V. K., and Minkowycz, W. J., "Heat Transfer from Fin-tube Radiators including Longitudinally Nonisothermal Surfaces," TN D-2077, 1964, NASA.

[3] Costello, F. A., "Analytical Prediction of Spacecraft Radiator Performance," Paper 65-WA/HT-45, Nov. 1965, American Society of Mechanical Engineers.

[4] Mendelsohn, A. R., "Contact Effectiveness of a Space Radiator," *Journal of Spacecraft and Rockets*, Vol. 2, No. 6, Nov.–Dec. 1965, p. 995

[5] Russell, L. D. and Chapman, A. J., "Analytical Solution of the 'Known-Heat-Load' Space Radiator Problem," *Journal of Spacecraft and Rockets*, Vol. 4, No. 3, March 1967, p. 311.

[6] Jakob, M., *Heat Transfer*, Vol. I, New York, Wiley, 1949, p. 233.

[7] Kays, W. M., *Convective Heat and Mass Transfer*, New York, McGraw-Hill, 1966, pp. 111 and 174.

[8] Spiegel, M. R., *Mathematical Handbook*, New York, McGraw-Hill Schaum's Outline Series, 1968.

Payload Optimization Factors for Storage of Liquid Hydrogen in a Low-Gravity Environment

A. L. SHERMAN*

McDonnell Douglas Astronautics—Western Division, Huntington Beach, Calif.

Nomenclature

c_p	=	specific heat at constant pressure, Btu/lbm − °R
Gr	=	Grashoff number = $\lvert B_g L^3 T/\nu^2 \rvert$
Bo	=	Bond number = gravity forces/viscous forces = $L^2 P_g/\sigma$
T	=	temperature, °R
MR	=	engine mixture ratio, $\dot{w}_{ox}/\dot{w}_{fuel}$
I_{sp}	=	specific impulse, sec
g	=	acceleration level, ft/sec^2
T	=	thrust, lbf
L	=	length, ft
W	=	weight, lb; w = flowrate, lb/sec
$\dot{w}$	=	flowrate, lb/min
P	=	saturation pressure; P_t = tank pressure, psia
k	=	thermal conductivity, Btu/ft-hr-°F
ρ	=	density, lb/ft^3
σ	=	surface tension, lbf/ft
μ	=	viscosity, lbm/hr-ft
ν	=	kinematic viscosity, μ/ρ
APS	=	auxiliary propulsion system

Introduction

MANY of the Apollo application missions and post-Apollo studies require orbital storage of cryogenic propellants; among these are such missions as the Saturn V Synchronous orbit, 110-hr, Lunar Applications Spent Stage (LASS) mission, and numerous orbital docking and propellant transfer experiments. During these periods in orbit, it will be necessary to vent the excess tank pressures (P_t) caused by

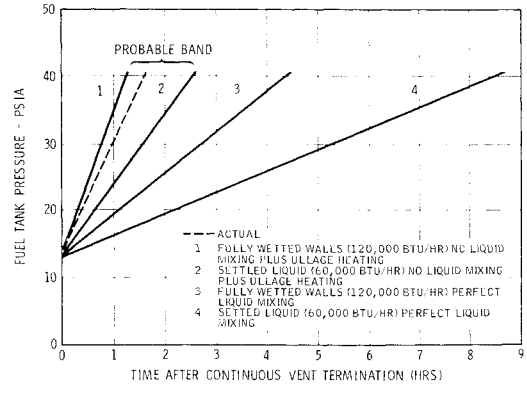

Fig. 1 Fuel tank (LH_2) pressure predictions (no venting).

Presented as Paper 69-1007 at the AIAA/ASTM/IES 4th Space Simulation Conference, Los Angeles, Calif., September 8–10, 1969; submitted September 2, 1969; revision received November 7, 1969. Phases of work presented herein depend partly on information supplied by Contract NAS7-101 by the McDonnell Douglas Astronautics Company—Western Division for NASA.

* Section Chief, Analytical Branch, Saturn Propulsion.

propellant boiloff. To accomplish venting, it will be necessary to position and maintain control of the propellants during the vent cycles. The present S-V LOR mission employs a continuous propulsive vent system during orbital coast for propellant control and removal of excessive propellant boiloff. In this concept, boiloff gas is used to maintain propellant control by venting the gas overboard in a propulsive manner axial to the stage.

The nature of the foregoing missions, however, precludes the uses of the continuous venting concept for control of propellants and venting of boiloff gas, because 1) frequent, precise maneuvers and docking techniques are involved which require minimal impulse disturbances from the stage during these critical periods, and 2) the amount of boiloff available for propellant control during continuous venting is insufficient due to the use of high-performance insulations to minimize propellant loss (large reductions in boiloff will be required for long missions to minimize tankage requirements).

It appears that a cyclic type of venting scheme will best suit the needs of these missions. Such a scheme would allow the propellants to "float freely" in a zero-g environment until such time as the heat input to the tank causes sufficient boiloff of propellants to raise the tank pressure to the maximum allowable value. At this time, a pressure switch would signal an external settling force to position, control, and maintain the propellants away from the vent system prior to venting. Then the tank would be vented to a safe P_i. The gases vented overboard in a propulsive axial mode would be utilized to maintain propellant control after the initial settling phase. During the venting period, proper procedures and/or liquid controls must be employed to eliminate or minimize liquid entrainment which is more pronounced at low-g levels.[1]

This Note discusses the factors that must be considered in order to optimize the conditions for orbital storage of liquid hydrogen (LH_2) and to determine payload advantages associated with these various conditions. Explicit parameters that were varied and compared include agitated vs stagnant liquid conditions, payload cost of providing agitation, influence of vent pressure settings, tank pressure history, and gravity level utilized for settling and control of propellants during venting.

At present, much remains unknown regarding orbital fluid dynamics and heat transfer. To date, studies indicate that very little mixing occurs in a low gravity environment. Comparisons of agitated vs stagnant LH_2 conditions are made on this basis, including the weight cost for providing agitation. The data from the SA-203 S-IVB orbital LH_2 experiment[2] were used as a basis for comparison with the model presented in this Note. Good correlation has been achieved with the predicted rise rates in the LH_2 tank using the stagnant model (Fig. 1).

The results presented herein depend strongly upon the model used, and extrapolation of these results to other conditions must be done with care. The techniques employed, however, can be modified for adaptation to other missions and conditions. The S-V LOR mission was chosen as a model because of its dominant role in present and near future mission planning.

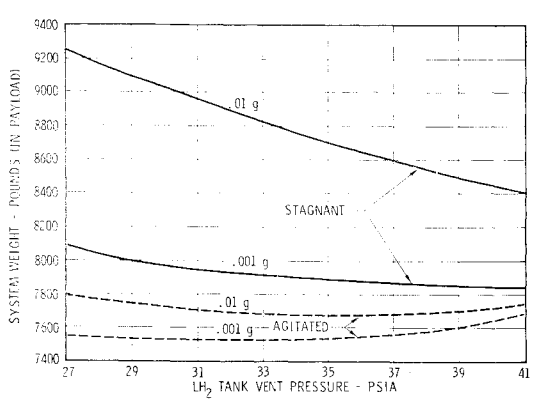

Fig. 2 Comparisons of total system weight (agitated vs stagnant).

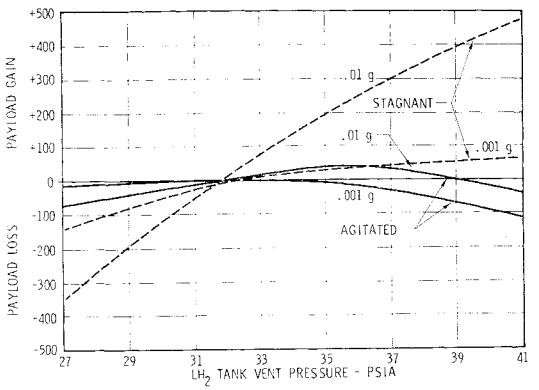

Fig. 3 Payload gain or loss associated with change in nominal vent settling.

Description of Model

An agitated or completely mixed fluid is defined as one with $k = \infty$. To ensure good mixing, it is necessary that certain conditions are satisfied. It was decided to use a minimum of 100 to insure a gravity-dominated condition and $Gr > 10^{10}$ to insure turbulent flow. The time between vent cycles for the agitated case may be determined by equating propellant heat capacity with the rate of incoming heat flux.

A stagnant fluid is defined as one with a finite k with negligible convection. Thus, extreme temperature gradients are formed throughout the liquid which depend on the fluid thermal diffusivity and heat transfer rate. The tank pressure rise rate is controlled by the vapor pressure of the high-temperature regions adjacent to the tank wall. Therefore, the time between vent cycles is determined by the temperature history of the surface fluid temperature (rather than the entire bulk) as a function of time. Thus, nearly all of the liquid bulk heat storage capacity, $WC_p\Delta T$, is unavailable. Here, ΔT is the temperature rise that corresponds to the maximum allowable saturation pressure rise.

The APS system is used for propellant positioning prior to venting. Thus, the system size is strongly dependent on the number of vent cycles and acceleration level utilized for settling.

Discussion

Over-all system weight change (whether agitated vs stagnant conditions or either of the two conditions separately at different pressures) is mainly a function of changes in boiloff,

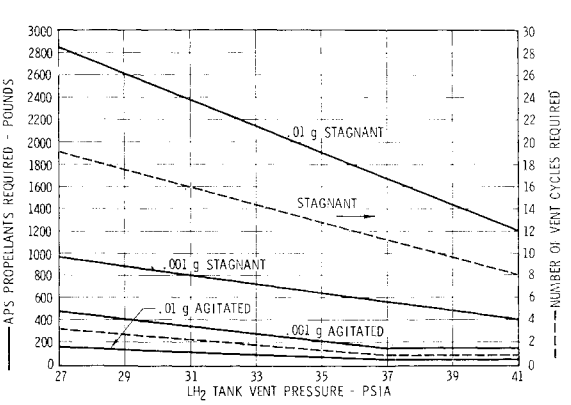

Fig. 4 Orbital vent cycle requirements and APS propellants required for venting.

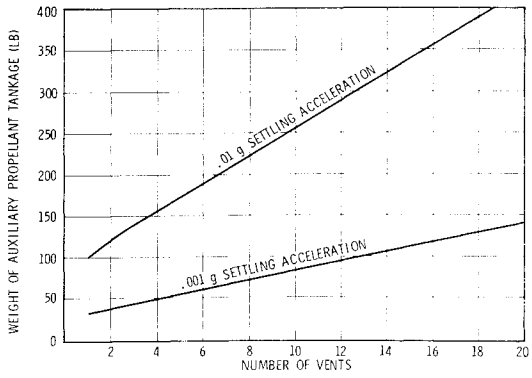

Fig. 5 Weight of ASS tankage.

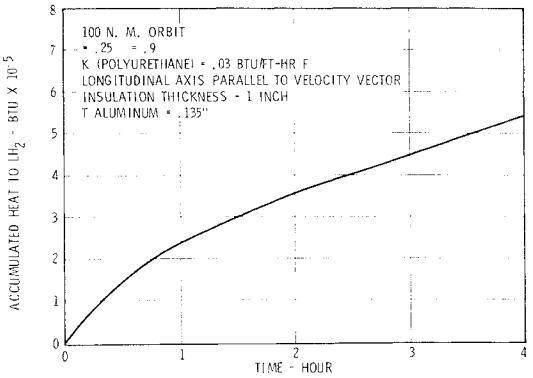

Fig. 7 Accumulated heat flow to the LH_2.

structural weight, pressurant, and auxiliary propellants, and tankage required for propellant positioning prior to venting. When comparing agitated-system weight vs stagnant-system weight (at the same tank conditions), the auxiliary propellant for providing LH_2 settling prior to venting is the dominant factor. For the 4.5-hr model presented, the stagnant condition requires from 7 to 17 more vent cycles (depending on vent pressure settings) than the agitated case, thus imposing a severe payload penalty on the stagnant condition. The system weight requirements for providing agitation do not appear inordinant compared to the considerable payload gains that can be realized by agitating the liquid. Thus, it appears desirable to make provisions to insure agitation (Fig. 2).

When parameterizing for the optimum operating pressures for the agitated or stagnant case individually, the payload gains and losses are not as well defined. For agitated conditions, the vent pressure setting has relatively little effect on payload (Fig. 3), because the structural requirement, which increases with higher P_t, is approximately offset by the saving in boiloff (due to the increased bulk heat capacity). When a significant reduction in vent cyles is involved, higher pressures are beneficial, but in the agitated case, this effect is small. The use of higher P_t for reasons related to NPSH or minimum engine start pressure would not cause appreciable payload penalties.

For the stagnant case, an increase in operating P_t will reduce the number of vent cycles considerably, especially at accelerations $\gg 0.001$ g, as shown in Fig. 3; this results in a significant reduction in system weight. However, the dominant weight factor is the auxiliary propellant required for settling the LH_2 during venting. This is due to the large number of vents required (Fig. 4).

The settling time varies as $(1/g)^{1/2}[g = f(T) = 2L/g]$ while $\dot{w}$ is directly proportional to $g[g = f(T) = \dot{w}I_{sp}]$. Thus, a reduction in g level from 0.01 to 0.001 g will result in an APS propellant reduction by a factor of 3.1 $(g_2/g_1)^{1/2}(g_1/g_2) = (g_1/g_2)^{1/2} = 10^{1/2} = 3.1$. However, until further low-gravity data are available on g forces required for settling and venting, 0.01 g will be used as the design criterion for this study.

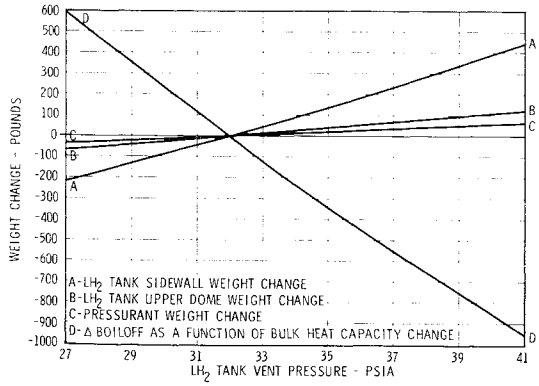

Fig. 6 Weight changes associated with vent setting variations (parameters independent of g level).

Results and Conclusions

The results of this study indicate that agitation of the LH_2 (including the cost of providing agitation) will yield definite payload gains when compared to stagnant LH_2 storage conditions, as shown in Fig. 2. The convergence of the curves for agitated and stagnant liquid conditions, as P_t increases, is due to the rapid decrease in vent cycles for the stagnant condition (propellants required for ullage settling is the dominant weight factor for the stagnant condition due to the large number of vents required when compared to the agitated condition). At extremely high pressures, venting should be eliminated (both stagnant and agitated), and over-all system weights would be identical.

Figure 3 shows that if agitated conditions prevail or are imposed, the effects of increasing the nominal vent setting are relatively insignificant, because of the accompanying increase in structural requirements and decrease in boiloff. For 4.5-hr coast mission, a maximum of 3 vents will be required for the agitated case while a maximum of 20 vents will be required for the stagnant case. This is indicative of the influence that auxiliary ullage settling propellants have on the over-all conditions. Changing the vent setting in the stagnant case has a much more pronounced effect. Figures 4–6 represent the various items that comprise the total system weight and the payload gains and penalties they impose.

Figure 7 presents the accumulated heat flow to the LH_2 and the associated properties of the insulation for the model used. This is typical for a Saturn V LOR mission and is substantiated by data from the various flights to date. Figure 8 represents typical pressure histories and numbers of vents required for the completely agitated and stagnant conditions based on the heat input history of Fig. 7. The stagnant condition is similar to that expected in a low-gravity

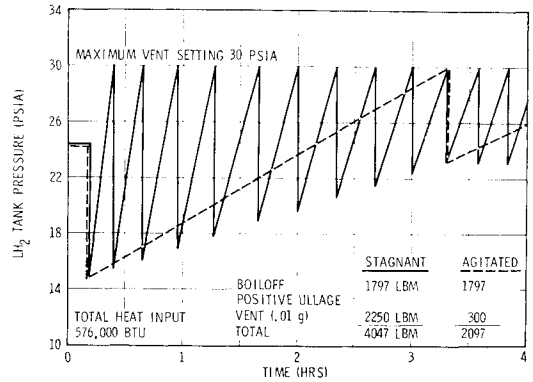

Fig. 8 Fuel tank pressure history.

environment as substantiated by the SA-203 orbital liquid hydrogen experiment and depicted in Fig. 1.

References

[1] Majoros, J. and Smith, D. A., "Control of Liquid Entrainment During Venting," *IES Proceedings, 1965*, DAC Technical Paper 3390, McDonnell Douglas Corp.

[2] "Saturn S-IVB-203 Stage Flight Evaluation Report," DAC-SM 46988, March 1967, McDonnell Douglas Astronautics Co., Western Div., Huntington Beach, Calif.

Solid-Propellant Grain-to-Mandrel Adhesion Phenomena

J. D. Burton*

Rocketdyne, A Division of North American Rockwell Corporation, McGregor, Texas

In structural evaluation of propellant grains for solid rocket motors, effects of the cure process are often loosely treated, using strain evaluation cylinder measurements to infer grain response to cure. With the advent of devices for monitoring grain-case bond line stress state during the life cycle of a solid-propellant motor,[1,2] experimental data indicating the influence of cure shrinkage in current standard processes have been generated. Volumetric shrinkage, due in part to polymerization of the binder material during cure, coupled with propellant-to-mandrel adhesion has been detected and gives cause for some concern as to its effect on the grain structural integrity. Observations that define the basic impact of the shrinkage on grain structural integrity and on the analytic evaluation of the integrity are described.

Experimental Observations

The test vehicle for this study was a set of 4-in. analogue motors cast with cylindrical port grains of Carboxyl-terminated polybutadiene(CTPB) propellant with web fractions on the order of 60% and instrumented with through-the-case type normal bond stress transducers, Fig. 1. No liner material was used in these motors. The mandrels used to form the inner port were Teflon†-coated rods after the standard method of motor processing. Tests were also conducted in which the mandrel was covered with tubegauze and the tubegauze covered with a latex membrane. This system, although impractical for real motors, provides a positive mandrel release. Bond line stresses for three motors during propellant cure, typical of the several tests conducted, are shown in Fig. 2. Motor A employed three curative systems to emphasize the effect of polymerization on the grain stress-state during cure. Motors B and C contained the same basic propellant with its standard single curative. Motor B was cast with a

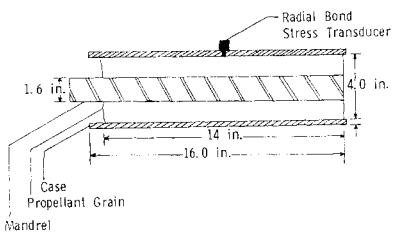

Fig. 1 Instrumented analogue motor.

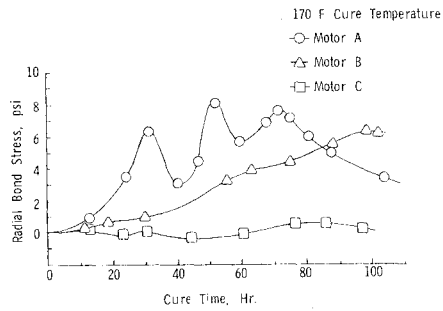

Fig. 2 Cure response.

Teflon-coated mandrel and motor C with the tubegauze-latex system.

Further emphasis on the relation between shrinkage and propellant adhesion to the mandrel is shown in Fig. 3. The response portrayed was measured in the first minutes of cool-down on completion of motor cure. The rapid rise in bond stress is indicative of a highly constrained, nearly incompressible material undergoing shrinkage. As propellant-to-mandrel unbond occurs, the stress is seen to relax in a pattern typical of viscoelastic materials. Motor C, with the positive release system, shows only the response of a cylindrical grain to thermal cool-down and follows the expected stress-time profile. Subsequent reheating of the motors to the cure temperature followed by the same environmental changes gave no spike and further indicated that the phenomena were due to propellant-to-mandrel adhesion.

Summary and Conclusions

In addition to the tests conducted specifically for identification of mandrel adhesion and the cure shrinkage process, observations made on full-scale motors[3] and on numerous strain evaluation cylinders further confirm the results described previously. Concern for the effect of mandrel adhesion stems from the uncertainties introduced by the observed phenomenon. The adhesion is an uncontrolled processing variation that may lead to decreased structural reliability. During the cure period, the propellant is undergoing a change of state and the normal volumetric shrinkage, if prevented by boundary constraints, must lead to the formation of voids or fissures within the grain. Finally, the analysis of the grain structure depends on an assumed stress-free starting point. This starting point is obviously not the end of motor cure and the analysis must, therefore, include the cure period. Insufficient data are available for rigorous analytical treatment of propellant behavior during cure but at least one approach has been proposed to define this behavior.[4]

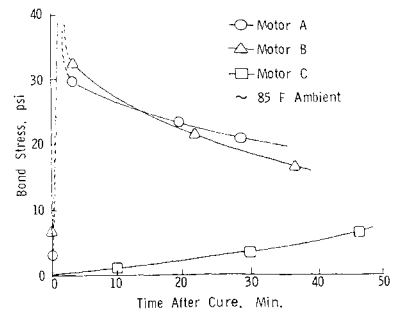

Fig. 3 Spiking phenomena.

References

[1] Burton, J. D., "Solid Propellant Grain-to-Case Bond Stress Measurement," presented at the SESA 1969 Fall Meeting, Houston, Texas, Oct. 1969.

[2] Leeming, H., "The Structural Test Vehicle as an Evaluation Tool for Propellant," AIAA Paper 68-508, Atlantic City, N. J., 1968.

Received October 6, 1969.

* Member of the Technical Staff.

† DuPont trademark for a tetrafluoroethylene plastic.